PCCP

XLPE based Al2O3/Clay Binary and Ternary Hybrid Nanocomposites: Nanoscale Hybrid Filler Self-Assembling, Polymer Chain Confinement and Transport Characteristics

Journal:	*Physical Chemistry Chemical Physics*
Manuscript ID:	CP-ART-07-2014-003403
Article Type:	Paper
Date Submitted by the Author:	30-Jul-2014
Complete List of Authors:	Jose, Josmin; Mahatma Gandhi University, School of Chemical Sciences Thomas, Sabu; mahatmagandhi university, School of Chemical Science

XLPE based Al_2O_3/Clay Binary and Ternary Hybrid Nanocomposites: Nanoscale Hybrid Filler Self-Assembling, Polymer Chain Confinement and Transport Characteristics

Josmin P. Jose[1 a], Sabu Thomas[1, 2 b*]

[1] School of Chemical Sciences, Mahatma Gandhi University, Kottayam, Kerala, India, 686 560

[2] International and Interuniversity Centre for Nanoscience and Nanotechnology, Mahatma Gandhi University, Kottayam, Kerala, India, 686 560

[a] josminroselite@gmail.com, [b]sabupolymer@yahoo.com

Abstract

Transport properties of hybrid nanoparticle based Cross-linked polyethylene (XLPE)/Al_2O_3/clay binary and ternary nanocomposites have been investigated with special significance to the hybrid effect and synergism of hybrid nanofillers. Compiling the temperature and filler effects, demonstrates the self-assembly of hybrid nanofillers in confining the polymer chain dynamics. Studies on transport mechanism, transport coefficients, & swelling parameters confirm the superior solvent resistant properties of hybrid filler reinforced nanocomposites. Experiments confirmed the extra stability of the ternary hybrid nanocomposites against the process of solvent penetration. Thermodynamic and kinetic investigations reveal that the nanofillers are competent to alter the thermodynamic feasibility and rate constant parameters. Theoretical predictions by Peppas Sahlin model suggest that the diffusion process is well thought-out to be the combination of diffusion into the swollen polymer and the polymer chain relaxation process. Morphology and the network density estimation confirms the presence of filler networks and the trapped polymer chains inside it, in ternary systems, which elucidate the micro structure assisted solvent resistant property of the ternary hybrid nanocomposites. The amount of polymer chains immobilized by the filler surface has been computed form dynamic mechanical analysis and a nice correlation was established between transport characteristics and the polymer chain confinement.

Key Words: Transport Characteristics, ternary hybrid nanocomposites, hybrid filler self-assembling, polymer chain dynamics, cross-linked polyethylene

1. Introduction

To prepare high-performance hybrid composites, the dispersion of inorganic fillers and the interfacial interaction between matrix and fillers are considered as the key issues. Hybrid reinforcements for polymer composites are getting increased acceptance, because they offer a range of properties that cannot be obtained with a single type of reinforcement. Two different filler types are used in the case of three-component compounding, which produces so called hybrid structures, in which, properties of different components are combined.[1] Hybridisation with more than one filler type in the same matrix provides another dimension to the potential

versatility to the parent system.[2] The super microstructure development associated with the synergism between the nano fillers leads to enhanced properties.[3]

The diffusion and transport in hybrid polymer nanocomposites depend upon the nature of the fillers, the degree of adhesion and their compatibility with the polymer matrix. If the filler used is inert and if it is compatible with the polymer matrix, it will take up the free volume within the polymer matrix and create a tortuous path for the permeating molecules. The degree of tortuosity is dependent on the volume fraction and the shape and orientation of the particles.[4] On the other hand if the filler is incompatible with the polymer matrix, voids tend to occur at the interface, which tends to increase the free volume of the system and thereby increases the permeability through it.[5] The interest in organic−inorganic hybrid nanocomposites is due to the fact that, the ultrafine or nano dispersion of filler, as well as the local interactions between the matrix and filler, lead to a higher level of properties.[6] Vlasveld *et al.*[7] observed that the diffusion in PA6 nanocomposites is at a slower rate than the unfilled PA6 specimens. The diffusion coefficients of the nanocomposites are reduced to approximately 1/3 rd of the original value at the highest silicate loading. The reduction in polymer chain mobility by the formation of a constrained region in nanocomposites also affects the diffusion characteristics. Restriction of polymer motion is a function of the interaction of the polymer with the surface of the nanoparticle. This is supported by observations of solvent uptake by Liang and Yin [8], Liang *et al.* [9], Singh and Mukherjee [10], on a number of nanocomposites. In each of these cases the solvent uptake decreased with increasing nanoparticle loading and was substantially lower than the solvent uptake of the pristine polymer.

Since Cross-linked polyethylene (XLPE) based materials are very important in the application fields of insulation, storage *etc.* it is recommended to investigate the transport characteristics of the system. In a complete hybrid system of organic/inorganic composites, there are two possibilities of solvent penetration: penetration of polar solvents like water, which will be facilitated by the polar inorganic component (nanofiller) and the penetration of non-polar organic solvents, which is favoured by the presence of major phase of non-polar organic polymer. Our previous experiments circumvent the possibility of water absorption by the nanocomposites even at high temperature. The non-polar organic polymeric major phase answers for this behaviour. In the case of organic solvents, major orgnic non polar polymer phase facilitates the penetration, but the minor phase of nanofillers is in opposition to the solvent penetration. Although the nanofillers are minor phase, it is in nanophase and well distributed throughout the XLPE matrix and can control the interphase and thereby the whole system. At room temperature the highly oriented semicrystalline polymer phase, which is more packed by the presence of nanofillers, resist the solvent uptake and thus solvent penetration is not possible at room temperature. It is worth to analyse the high temperature transport behaviour of hybrid nanocomposites (where the semicrystalline phase undergo melting) with organic solvents and a comparison of different performance levels of binary and ternary systems of nanocomposites.

In this study the transport of organic solvent toluene through the XLPE/Al_2O_3/clay hybrid nanocomposites has been investigated in detail with special reference to the hybrid effect of nanofillers. Experiments established the extra stability of the ternary hybrid nanocomposites against the process of solvent penetration by the altered microstructure through the synergism of nanofillers. The present study is the first attempt to evaluate the diffusion characteristics of nanocomposites of XLPE continuous phase with combination of different nanofillers where hybrid fillers self-assemble to form a network where polymer chains are immobilized. The diffusion characteristics of binary and ternary hybrid nanocomposites of XLPE has been compared in correlation with the micro structural development and polymer chain dynamics in binary and ternary systems. Morphology and the network density estimation confirm the presence of filler networks and the trapped polymer chains in ternary nanocomposites, which elucidate the micro structure assisted superior solvent resistant property of the ternary hybrid nanocomposites.

2. Experimental

2.1 Materials

Low density polyethylene (PETROTHENE NA951080), density 0.94 g/cm^3 was obtained from Equistar, United States. The cross linking agent dicumyl peroxide (DCP) and antioxidant Irganox were used. The nano Al_2O_3 with 100 % silane, trimethoxyoctyl-reaction product, and nanoclay: Bis(hydrogenated Tallow Alkyl)dimethyl, ammonium salt with Bentonite were obtained from Evonik Industries, United States.

2.2 Nanocomposite Fabrication

XLPE/Al_2O_3/clay hybrid ternary composites of Al_2O_3 and clay in 1:1 and 2:1 composition, binary composites of XLPE/Al_2O_3, XLPE/clay composites were prepared by melt mixing using dicumyl peroxide as the curing agent. The cross linking agent, DCP 1.5 wt% and antioxidant 0.5 wt% were used. The mixing was done in a Haake mixer at 160 ^oC and 60 rpm for 12 minutes. The temperature, rotation speed, time of mixing and the amount of DCP and Irganox were kept constant for all mixes. The mixed nanocomposites were compression molded in a SHP-30 model hydraulic press with a maximum pressure of 200 kg/cm^2 at 180 °C for 5 minutes. High pressure was applied while moulding, otherwise the escaped methane, the cross linking by-product will form pores in the films. For all nanocomposites, the nanofiller concentration was kept fixed as 5 wt% and XLPE/Clay composite is designated as C, XLPE/ Al_2O_3 composite is designated as A, Al_2O_3: clay = 1:1 composite is designated as A1C and Al_2O_3 : clay = 2:1 composite is designated as A2C. Composite of XLPE without nanofiller, designated as X was also prepared for comparison.

2.3 Nanocomposite Characterizations

2.3.1 Transmission Electron Microscopy (TEM)

The dispersion of nano fillers in polymer nanocomposites was investigated using TEM. The micrographs of the nanocomposites were taken in JEOL JEM transmission electron microscope with an accelerating voltage of 200 keV. Ultrathin sections of bulk specimens (about 100 nm thickness) were obtained at -120 ^{o}C using an ultra-microtome fitted with a diamond knife.

2.3.2 Diffusion Studies

Circular samples (diameter ≈ 2 cm) of ASTM standard D5890 were weighed and immersed in toluene contained in test bottles with airtight stoppers. The experiments were done at 3 different temperatures of 70, 80 and 90 ^{o}C. At the expiration of the specified time, the samples were removed from the sample bottles, wiped free of adhering solvent and weighed using a high resolution electronic balance. The weighing was continued till equilibrium solvent uptake was attained. Each weighing was completed at the earliest, so as to decrease the error due to solvent evaporation from the sample surface.

2.3.3 Dynamic Mechanical Analysis

Dissipation factor was analysed in shear mode using Home-made machine in MATEIS, INSA de Lyon, France. Rectangular samples at frequency 1 Hz, angle 10^{-2}, couple range 10^{-5} to 10^{-8} were tested. Temperature range of 100 K to 200 K at 1K/minute used for the experiment. Liquid N_2 atmosphere is used to reduce the temperature to 100K.

2.3.4 Tensile Tests at 120 ^{o}C

Tensile tests were performed at 120 ^{o}C to estimate the network density of the system using EOLEXOR 500 N/Auto sampler (ASSS) (GABO Qualimeter Testanlagen Gmbh) machine. The dumbbell shaped samples of with 10 mm length in between clamps were used. The span length and cross head speed used for the testing were 40mm and 50mm/min, respectively. From the stress-strain behaviour, above the melting temperature (at 120 ^{o}C), the modulus value could be attained. This modulus value will be the direct result of the network structure of the system, as the crystalline fraction melts at this temperature, which is the main contributor of the modulus value of a semi crystalline polymer below its melting temperature.

3. Theoretical Background of Transport Characteristics

Diffusion Characteristics: The results of solvent uptake by the polymer are expressed as mol % of the solvent absorbed by 0.1kg of the polymer (Q_t). The solvent uptake (Q_t (%)) of the samples was computed using the equation,

$$Q_t(\%) = \frac{m_t - m_0}{m_0} x100 \quad \ldots\ldots(1)$$

Where m_0 and m_t are the weights of samples before and after a time t of immersion.

Mechanism of Transport: In order to investigate the type of transport mechanism, the sorption results were fitted into the following equation [11]

$$\log \frac{Q_t}{Q\alpha} = \log k + n \log t \quad \ldots\ldots(2)$$

Where Q_t and Q_∞ are the mol % solvent uptake at time t and at equilibrium respectively and k is a parameter which depends on the structural characteristics of the polymer in addition to its interaction with the solvent. The value of n indicates the type of the mechanism.[12] The value of n=0.5 indicates Fickian transport, while n = 1 shows case II (relaxation controlled) transport. The values of n between 0.5 and 1 indicate an anomalous mode of transport. Also there have been reports of n > 1 which is called super case II.[13] The values of n and k for all samples in the three solvents at room temperature were determined by regression analysis of the linear portion of plots log (Q_t/Q_∞) versus log t. To assure linearity, the values up to 50% of the equilibrium uptake were only used.

Transport Coefficients

(a) Diffusion Coefficient (D): The diffusion coefficient (*D*) is a kinetic parameter, which depends on the polymer segmental mobility, gives an indication of the rate at which a diffusion process takes place. It is the rate of transfer of the diffusing substance across unit area of cross section divided by the space gradient of concentration.[14]
The diffusion coefficient or the diffusivity D of a solvent molecule through a polymer membrane can be calculated using Eq. [3] obtained using Fickian's second law [15]

$$D = (h\,\theta/4Q_\alpha)^2 \quad \ldots\ldots(3)$$

Where h is the thickness, θ is the slope of the initial linear portion of the plot of % Qt against$\sqrt{t}$, and Q_α is the equilibrium absorption.

(*b) Sorption Coefficient:* The permeation of a penetrant into a polymer membrane depends on the diffusivity as well as on the sorption. Hence sorption coefficient is calculated using the Eq. [4]

$$S = \frac{M_\infty}{M_0} \quad \ldots\ldots(4)$$

Where, M_∞ is the mass of the solvent at equilibrium swelling and M_0 is the initial polymer mass.[16]

(c) Permeability Coefficient (P): Permeation can be considered as the combination of sorption and diffusion processes. The permeability coefficient (*P*) gives an idea about the amount of solvent permeated through uniform area of the sample per second.[17]
The permeability coefficient (P) can be obtained as follows: [18]

$$P = D * S \quad \text{.....(5)}$$

Where D is the diffusion coefficient and S is the sorption coefficient.

Swelling Parameters: The extent of swelling, interface strength and degree of dispersion of fillers in the polymer matrix can be inferred from the swelling parameter value.[19] The swelling coefficient can be estimated from the Eq. [6] [20]

(a) $Swelling\ coefficient = [(M_\alpha - M_o)/ M_o] \times \rho_s) \quad \text{.....(6)}$

Where Mo and Mα are mass of the sample before and after swelling, respectively, and ρ_s is the density of the solvent. Swelling index, which is another parameter of transport properties is calculated by the Eq. [7]

$$(b)\ Swelling\ index = [(M_\alpha - M_o)/M_o] \times 100 \quad \text{.....(7)}$$

Thermodynamic Parameters: The thermodynamic phenomena associated with the process of swelling are (a) an increase of entropy of polymer/solvent matrix by the introduction of small molecules as diluents and (b) a decrease of entropy of polymer by isotopic dilation. The entropy of polymer–solvent matrix is actually the entropy of mixing between polymer and solvent molecules. The mixing acts as the driving force for swelling. The thermodynamic functions ΔS, ΔH, ΔG were calculated by linear regression analysis using the Van't Hoff equation:

$$Ln\ k_s = \Delta S/R - \Delta H/RT \quad \text{.....(8)}$$

Where k_s is the thermodynamic sorption coefficient [21], ΔG is the free energy change, ΔS is the entropy of sorption and ΔH is the enthalpy of sorption. From the slope and intercept of the least square fit of the linear plot of log k_s against $1/T$ one can obtain the values of ΔS, ΔH and ΔG using the relationship:

$$\Delta G = \Delta H - T\Delta S \quad \text{.....(9)}$$

Transport Kinetics: The kinetics of transport of solvents through nanocomposites was studied by first order kinetics. The first order equation is

$$k_1 t = 2.303 \log \frac{C_\infty}{(C_\infty - C_t)} \quad \text{.....(10)}$$

Where, k_1 is the first order rate constant, C_t and C_∞ represent concentrations at a time t and at equilibrium. Plot of log (C_∞-C_t) versus time will give the rate constant k.

4. Results and Discussion

4.1 Morphology: High Resolution Transmission Electron Microscopy

High Resolution Transmission Electron Micrographs presented in Figure 1 demonstrate the filler distribution of different nanofillers in XLPE matrix. It is noted that, the network formed with the mixed fillers (Figure1c) demonstrates a complex microstructure of multiple clay bridging with adjacent alumina particles. This kind of effective networking occurs only in Al_2O_3:clay = 1:1 system. For Al_2O_3: clay = 2:1, alumina aggregation dominates over hybrid effect in network formation. XLPE/Al_2O_3 exhibits aggregation tendency, while XLPE/clay composite shows nice intercalated/exfoliated (mixed mode) structure. Since the natural structure, degree of dispersion and proportions of the fillers in ternary system are different, the morphology displays diverse features. The interaction between the surface treatment on the alumina nanoparticle and the organic modification on clay platelet may take part in the alignment of hybrid fillers and thereby effective network formation. In addition, the interaction between alumina and clay not only altered the composite morphology and filler dispersion but also gave rise to unique filler architecture.[22] In Figure 2, TEM images of A1C at different resolutions are given to confirm the predominating effect of hybrid filler alignment, especially in Figure 3C, it can be seen very clearly the interacting Al_2O_3 particles and clay platelets, which is the root cause for the self-assembly and consequent the network designing in the hybrid system of 1:1 ratio. As the surface energy and surface characteristics of both the fillers are different, aggregation tendency is minimized between these hybrid nanomaterials. For each combination of hybrid filler systems, there was an optimal volume ratio between the hybridising fillers. If the volume ratio of clay is too low, the limited number of fillers restricts the degree of bridging between alumina nanoparticles, as in the case of Al_2O_3:clay=2:1 system. Leung *et al.*[23] have reported a similar system, in which the bridging capacity of Boron nitride platelets with MWCNT and there by the formation of a structured network is investigated.

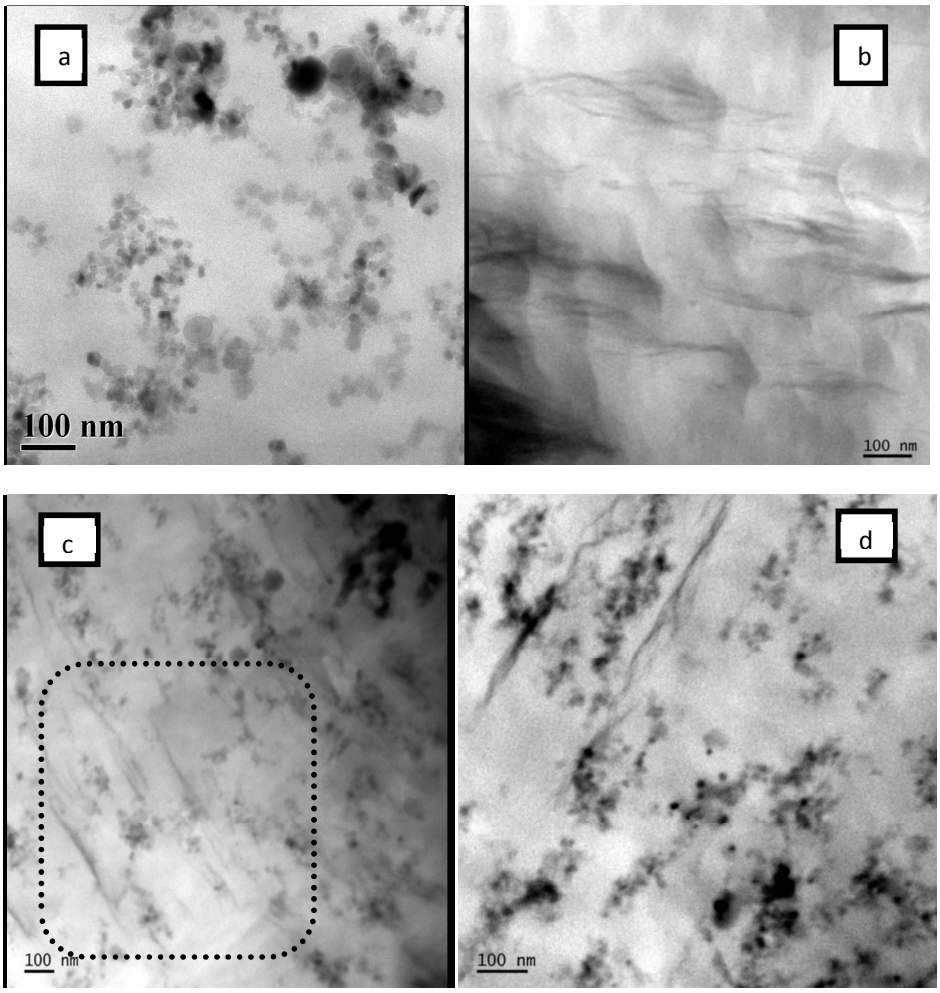

Figure 1 : Transmission electron micrographs of XLPE/ Al_2O_3 (a), XLPE/clay (b), XLPE/ Al_2O_3:clay=1:1 (c), Al_2O_3:clay=2:1 (d)

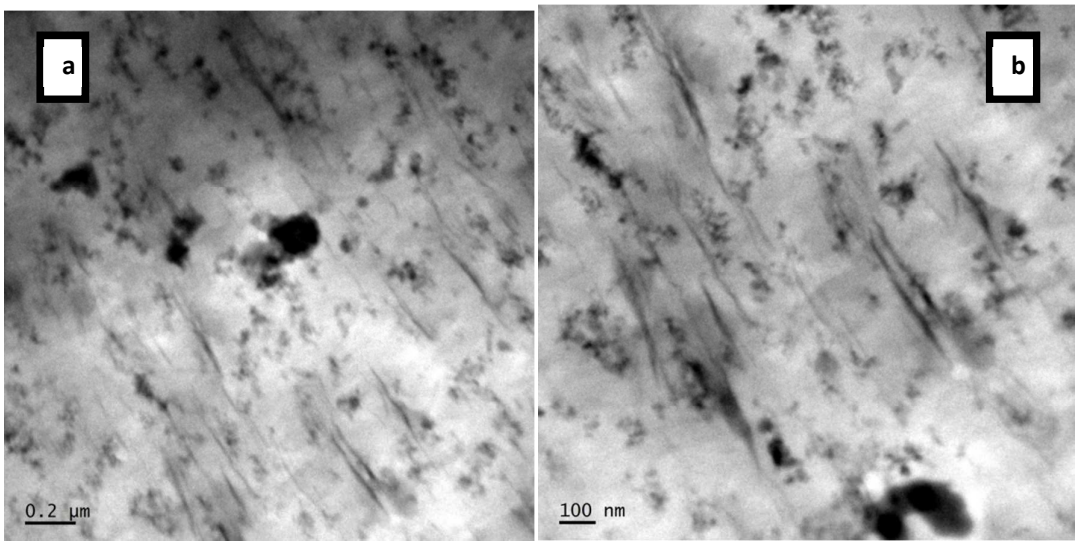

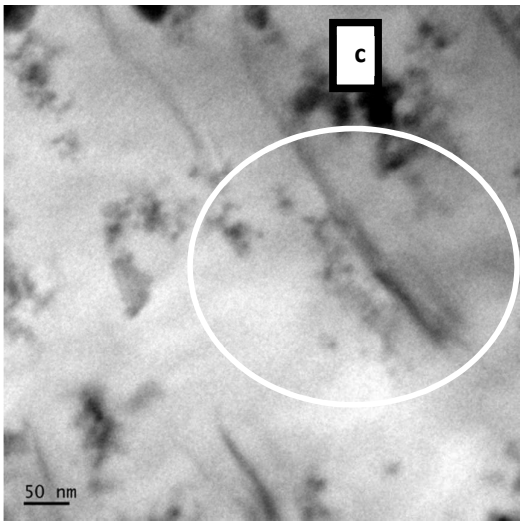

Figure 2 : Transmission electron micrographs of A1C at différent résolutions

4.2 Diffusion Characteristics

Figures 3, 4 & 5 present the solvent uptake as a function of time for three different temperatures, 70, 80 and 90 ^{o}C. The neat XLPE sample showed maximum uptake owing to the increased segmental mobility and availability of maximum free volume as compared to the filler-loaded system. As shown in figures, it can be seen that the initial swelling rate is too high in all the systems because of the large concentration gradient. As time goes on, the solvent uptake of the polymer samples decreases, owing to the decrease in concentration gradient and finally reaches the equilibrium swelling. The rate of sorption and maximum solvent uptake increases with the increase in temperature for all the samples. This can be attributed to the increase in free volume as a result of the increase in segmental motion of the polymer matrix as well as the gain in kinetic energy by the solvent molecules which resulted in an increased number of collisions.

The addition of nano fillers decreases the solvent transport dramatically. This can be explained based on the fact that the local mobility of the polymer gets restricted by reinforcement of nanofillers and improves the solvent resistance. Thus, the reinforcement by nanofiller improves the solvent resistance to a good extent. A higher material volume and higher flexibility of the network allow an increased solvent uptake for the unfilled sample. We can see two distinguished zones in the curves. The first zone corresponds to the initial solvent uptake. The swelling rate is too high in this area because of the large concentration gradient and the polymer sample is under severe solvent stress. The second zone indicates a reduced swelling rate due to the decrease in concentration gradient, which finally reaches at equilibrium swelling. This means that the concentration gradient attaining zero value.[24] Since PE is a semicrystalline polymer, there is no solvent uptake at room temperature. At high temperature regions, polymer chain mobility increases and the crystalline structure destruction occurs. In that case solvent molecules penetrate into the polymer matrix and the diffusion happens. While comparing the three temperatures of 70, 80 and 90 ^{o}C, solvent uptake is directly proportional to the temperature for the neat XLPE and the nanocomposites. Even at high temperature, nanocomposites are able to resist the solvent penetration to the

XLPE very effectively. The effect of nanofillers in blocking the solvent molecules is effective in all temperature regions. Even at 90 ^{o}C, system is very close to its melting, nanofillers are able to hinder the chain mobility and thus the diffusion process. The difference in solvent uptake at 80 and 90 ^{o}C is not very high, but for 70 and 80 ^{o}C is quiet high. Once the system is at 80 ^{o}C, chains start to move rapidly and further increase in temperature adds more free movements to the chains. But for 70 ^{o}C, the temperature was not sufficient to penetrate the solvent into a packed crystalline structure.

While comparing different nanocomposites of same filler concentration, solvent uptake is least for Al_2O_3/clay (1:1) ternary hybrid nanocomposite A1C. In hybrid composites, effective filler/filler networks can trap the polymer chains and thus the polymer segmental mobility will be reduced to a large extent. Also, due to the synergism of nanofillers of Al_2O_3 and clay, filler networks are strong and the polymer/filler interaction is also superior.[25] This will reduce the amount of free volume in ternary hybrid composites, which favours, its solvent resistant nature. For Al_2O_3:clay = 2:1 system, the micro structural limitation of dispersion due to the aggregation of alumina particles, reduce its solvent resistance.[26] The binary systems of XLPE/Al_2O_3 and XLPE/clay, exhibit less solvent uptake compared to the neat XLPE. In these systems, XLPE/Al_2O_3 is more efficient in resisting the solvent penetration than that of XLPE/clay nanocomposite. Since Al_2O_3 is a 3D spherical nanofiller, the surface area which is in contact with polymer is too high and thus it is more efficient in controlling the polymer chain dynamics. For 70 and 80 ^{o}C, the binary compound A exhibits higher value than that of ternary system of A2C, but at 90 ^{o}C it is just opposite. For Al_2O_3:clay = 2:1 system, the micro structural limitation of dispersion due to the aggregation of alumina particles, reduces its networking efficiency and which leads to a more inhomogeneous phase compared to A which is evenly distributed due to the surface treatment on Al_2O_3 particles. At 90 ^{o} C almost all the nanocomposites exhibit same values and A2C is slightly higher than that of A. At 90 ^{o} C, the polymeric system approaches melting and the polymer chain mobility is highly enhanced. Only the trapped polymer chains in the polymer networks have more resistance at this higher temperature. Although the volume of the trapped polymer chains is less, this trapping mechanism explains higher Qt value of A2C compared to A at 90^{o}C.

The Q_α as a function of different filler types is given in Figure 6. From the graph, it can be confirmed that the addition of filler helped the polymer to become more solvent resistant especially with the addition of hybrid fillers of Al_2O_3 and clay. This fact is again deep-rooted from the establishment of the correlation between normalized Q_α for different filler types at 70 ^{o}C (Figure 7). The effect of filler networking on diffusion characteristics is schematically represented in abstract graphic. The filler networks in ternary hybrid system can effectively block the diffusion process compared to the binary systems of nanocomposites by the effective self assembling of hybrid fillers as filler networks.

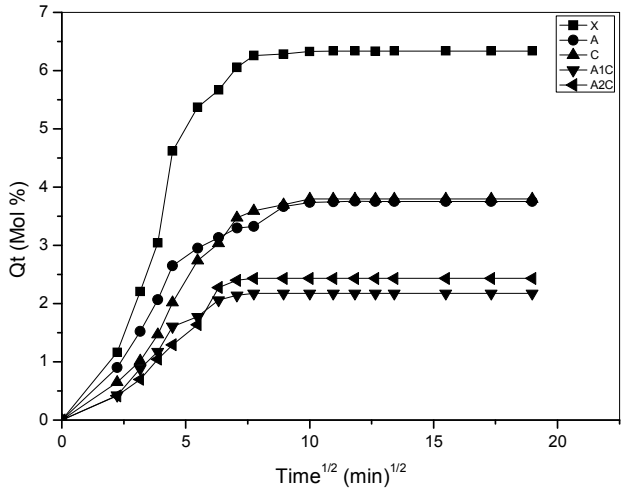

Figure 3: Q_t versus time ($min^{1/2}$) of XLPE/Al_2O_3/clay nanocomposites of 5 wt% filler concentration (at 70 ^oC) showing the transport through binary and ternary (hybrid) systems

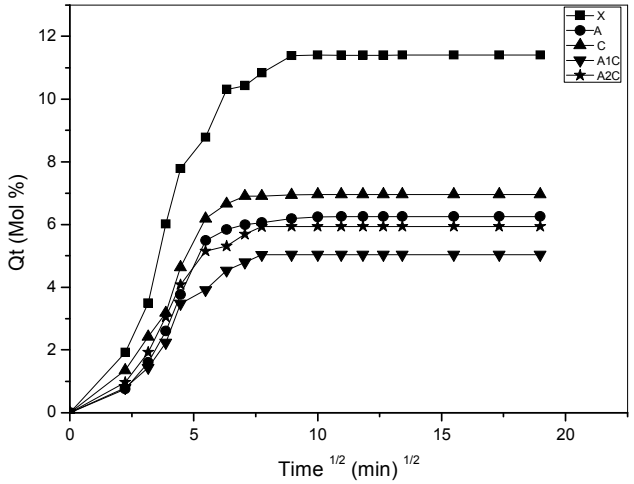

Figure 4: Q_t versus time ($min^{1/2}$) of XLPE/Al_2O_3/clay nanocomposites of 5 wt% filler concentration (at 80 ^oC) showing the transport through binary and ternary (hybrid) systems

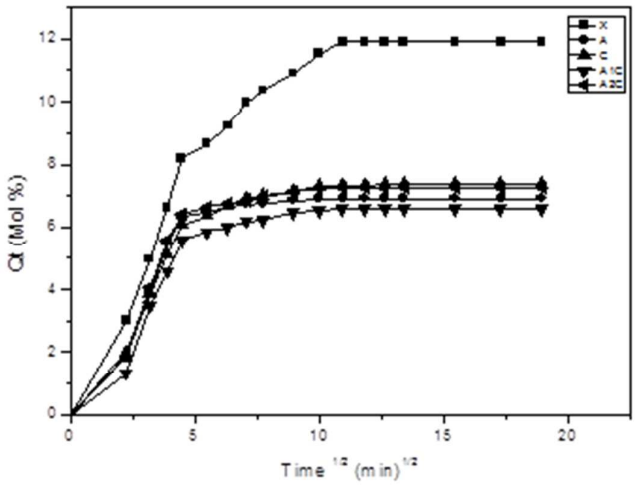

Figure 5: Q_t versus time ($min^{1/2}$) of XLPE/Al_2O_3/clay nanocomposites of 5 wt% filler concentration (at 90 ^oC) showing the transport through binary and ternary (hybrid) systems

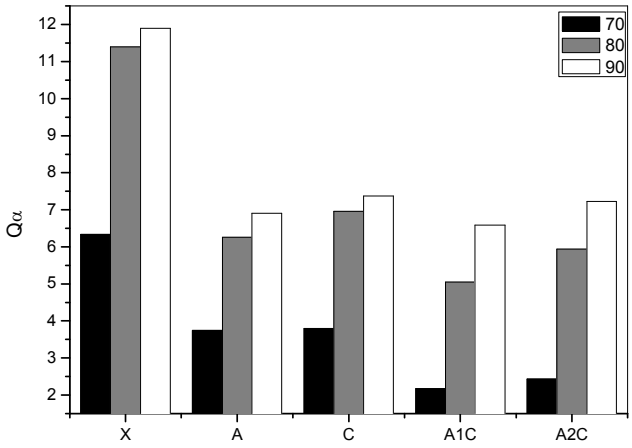

Figure 6: The Q_α as a function of different filler types at different temperatures

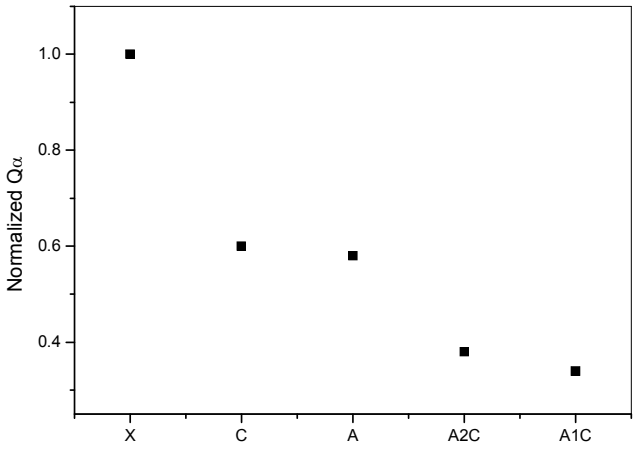

Figure 7: The normalized Q_α as for different filler types at 70 ^oC

4.3 Polymer Chain Dynamics: Estimation of Constrained Region

The temperature effect on diffusion behaviour can be further explained by the polymer chain dynamics in the vicinity of nanofillers. It is postulated that the high degree of reinforcing action and polymer chain confinement in the case of nanocomposites is associated with the formation of a constrained polymer layer around the filler surface, due to the efficient polymer/filler interaction. Interfacial interaction leads to the formation of effective nanophase and this immobilises the surrounding polymer chains. There is an effective constrained length around the nanfillers, and polymer chains lose their mobility, when the polymer chain is within this constrained length. The constrained region can be estimated from the height of the dissipation factor values of dynamic mechanical analysis.

Variation in dissipation factor (ratio of loss modulus to storage modulus) as a function of temperature with different nanocomposites are plotted in Figure 8. It can be seen that the height of the tan δ peak (glass transition) decreases with the addition of nanofillers. This implies that, the mobilization of macromolecules was restricted due to the addition of nanophase. Reduced chain mobility owing to physical and chemical adsorption of the polymer chain segments on the filler surface causes a height reduction of tan δ peak during dynamic mechanical deformation. The decrease in tan δ peak proves minimum heat build-up as a result of lesser damping characteristics for the compounds containing nanofillers. The height depression in the tan δ peak indicates that there is a reduction in the amount of mobile polymer chains during the glass transition and hence it can be used to estimate the amount of constrained chains.[27] According to Rao and Pochan [28], in polymer–clay nanocomposite, the nanoparticles create crosslinking of the matrix by interacting strongly with the polymer chain and limiting the mobility of surrounding chains. There is an effective constrained length around the nanfiller, and polymers lose their mobility during glass transition when the polymer chain is within this constrained length.[29] The depression in tan delta peak is

considerable for A1C sample compared to other systems. The arrested polymer chains in filler networks explain the constrained region in ternary hybrid nanocomposites and this is schematically represented in Figure 9. The only slight decrease in tan delta value is owing to the viscoelastic energy dissipated as a result of filler–filler friction and filler–PE interaction. The molecular mechanism of this relaxation in PE is quite complex and it is attributed it to the deformation of amorphous regions as a result of reorientation within crystallites. The constrained length in each sample can be estimated from the height of the tan delta peak.

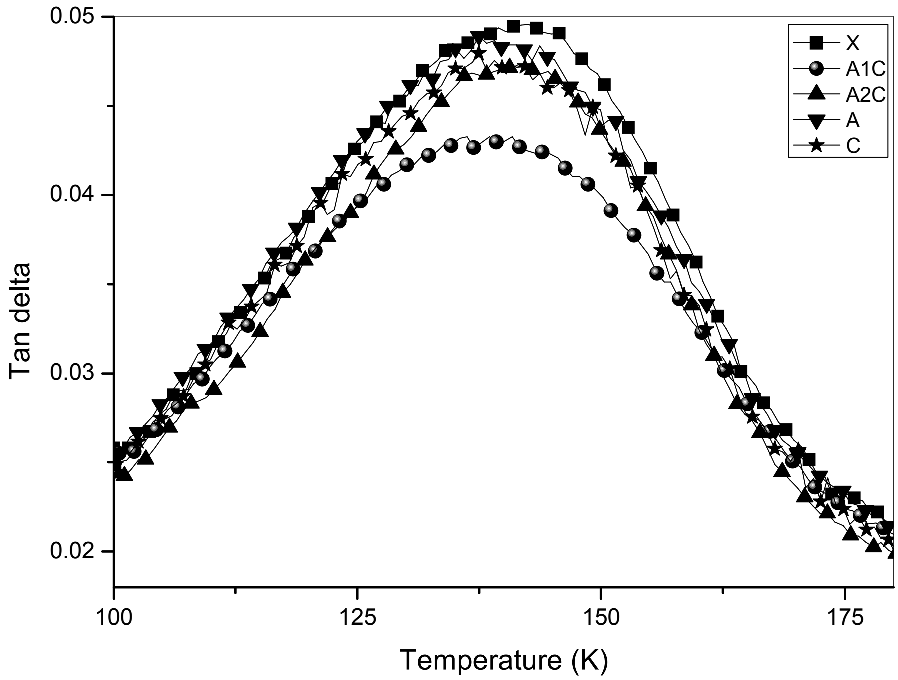

Figure 8: The tan δ values of XLPE and nanocomposites

For linear viscoelastic behavior, the relationship among the energy loss fraction of the polymer nanocomposite (W) and tan δ is given by the following equation

$W = \pi \tan\delta / (\pi \tan\delta + 1)$ ………………………………………………………….*(11)*

The energy loss fraction W at the tan δ peak is expressed by the dynamic viscoelastic data in the form.

$W = [(1- C) W_0] / (1-C_0)$ ………………………………………………………......*(12)*

Where C is the volume fraction of the constrained region, W_0 and C_0 denote the energy fraction loss and volume fraction of the constrained region of neat XLPE. This equation can be rearranged as follows.

The volume fraction of the constrained region, C is given by

$C = 1 - [(1-C_0)\, W / W_0]$ ……*(13)*

C_0 is taken to be 0. The height of the tan δ peak is used to calculate W according to Eq. (11) The estimated constrained region is given in Table 1.

Table 1: Estimated constrained region of nanocomposites

Sample	Constrained region (C)
X	-
A	0.045
C	0.055
A1C	0.132
A2C	0.054

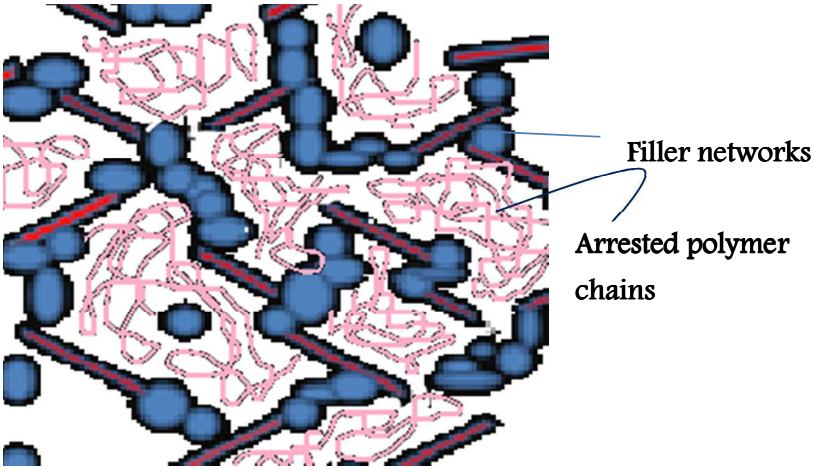

Figure 9: Schematic representation on effect of hybrid filler networks on polymer chain dynamics (circles represent spherical nano Al_2O_3 and rods represent nano clay)

The correlation between Qα and constrained region of different nanocomposites is shown in Figure 10. From the graph it is very clear that the amount of constrained region has a very good control over the Qα values by arresting the polymer chain dynamics in a considerable quantity. For the hybrid system of 1:1 ratio, the filler assembling and thus the filler networks are highly effective and which cause a good amount of constrained region and very low value of Qα. This behaviour of correlation between the Qα and constrained region explains the very clear picture of structure-property correlation and the role of chain dynamics in diffusion characteristics of binary and ternary hybrid nanocomposites.

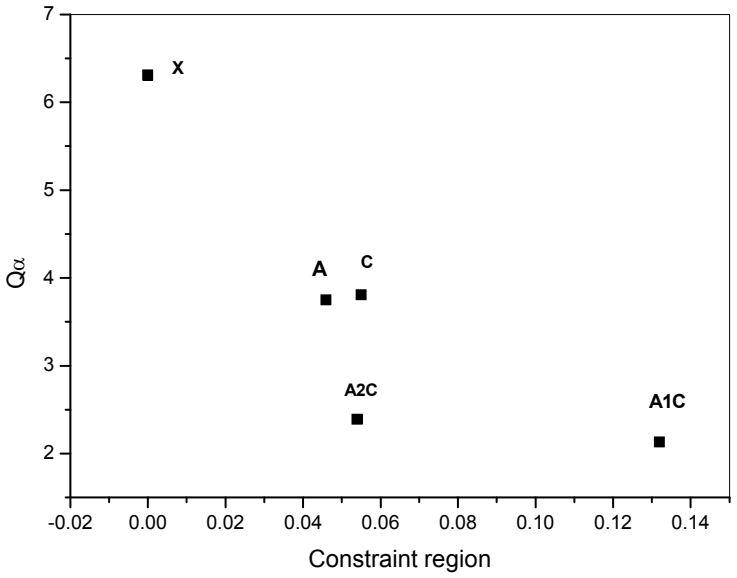

Figure 10: Correlation between Qα and constrained region of different nanocomposites

4.4 Mechanism of Transport

The n and k values of neat XLPE and different nanocomposites of 5 wt% filler concentration are calculated using Eq. 2 and the values are compared in Table 2. The n values are in the regions of $n > 1$ for X, A and A1C and $n < 1$ for the C and A2C systems. The $n > 1$ is super case II or relaxation-controlled transport and this situation occurs where the penetrant moves at a faster rate than the polymer relaxation process.[30] For a semicrystalline material rotation about the chain axis is limited and motion within the structure is largely vibratory within a frozen quasi lattice. These dense structures have very little void space (0.2 -10 %) too.[31] The time taken by polymer segments to respond to swelling stress and rearrange them to accommodate the solvent molecules is very high in the present system of XLPE. The polymer chains are tightly packed in XLPE and the networking is even more in nanocomposites. The surface treatment (long alkyl chain) on the alumina particle make a strong interaction between the polymer and nanofiller. In this situation the chain rearrangement is slow and the n values are in the range of $n > 1$. But for the clay filled composite, the interaction between clay and XLPE is weak in two ways compared to nano alumina. Since clay is nano dimensionally 2D, its surface area of interaction is less and additionally, the absence of surface treatment on surface of clay reduces its interaction with XLPE. Also for A2C system, due to the excess amount of alumina particles, effective networking is not happening or the filler networks are weak.[32] In both these cases, polymer chain rearrangement will be easier and the mechanism of transport is coming under anomalous domain and it happens when the mobility of the permeant molecule and the segmental mobility of the polymer are almost similar. The polymer/solvent interaction parameter k is less for all nanocomposites compared to the neat sample. The higher k values (*i.e.* the extent of polymer–solvent interaction) is the direct result of the absence of effective polymer–filler interaction. The k values of different

nanocomposites confirm the ability of nanofillers to fix the polymer chains, and thus reduce its mobility as mentioned above.

Table 2: The n, k values of XLPE and different nanocomposites at 5 wt% filler concentration

Sample	n	k
X	1.02	1.50
A	1.12	1.25
C	0.86	1.31
A1C	1.04	1.39
A2C	0.96	1.44

4.5 Transport Coefficients and Swelling Parameters

The transport coefficients: diffusion coefficient, sorption coefficient and permeation coefficient of XLPE and nanocomposites are shown in Table 3. As expected, all the transport coefficients are less for nanocomposites compared to the pristine XLPE. These values confirm the superior solvent resistance property of the nanocomposites, *i.e.* lower rate of diffusion, less the extent of sorption and less the amount of solvent permeated through the nanocomposites.[33] In different nanocomposites A1C is the best system which has the lowest diffusion coefficient, sorption coefficient and permeation coefficient values. This again supports the stability of the A1C composite against the solvent penetration process.

The result shows that the barrier properties of XLPE/inorganic nanocomposites are remarkable. Due to the nanometric level dispersion of the organic and inorganic phases, the available free volume decreases and the presence of nanofiller results in an increase in tortousity of the path which leads to the reduced diffusivity. A small diffusion coefficient indicates that only a small amount of solvent can be absorbed by the sample. The sorption coefficient shows a decreasing trend for nanocomposites which is a thermodynamic parameter, depends on the strength of the interactions in the polymer/penetrant mixture. The permeation coefficient follows the same trend of diffusion coefficient and so diffusion process controls the permeability. Permeation can be considered as the combination of sorption and diffusion processes.

Table 3: The diffusion coefficient, sorption coefficient, permeation coefficient and swelling parameters of XLPE and nanocomposites of 5 wt% filler concentration

Sample	Diffusion Coefficient $DX10^{11}(m^2/minute)$	Sorption coefficient g/mol	Permeation Coefficient $Px10^{10}(m^2/minute)$	Swelling coefficient (β)	Swelling index (%)
X	2.27	11.50	2.60	9.11	1050
A	1.23	6.76	0.83	4.99	576
C	1.52	7.41	1.13	5.55	641
A1C	1.03	5.65	0.62	4.03	464
A2C	1.29	7.58	0.976	4.83	558

Anisotropic swelling studies provide information on the interface strength, degree of dispersion of fillers and their alignment in the polymer matrix.[34] Swelling parameters represent the extent of swelling in the system, which are listed in Table 2. Swelling parameters are substantially lower for the nanocomposites, confirm their resistance towards swelling process. The reduced swelling is due to the enhanced interfacial bonding between the filler and polymer. This prevents the transport of solvent to a greater extent through the interface.[35] The presence alkyl groups on nanofillers by surface treatment can provide effective interaction between polymer and filler and thus the interface is strong enough to resist the swelling mechanism. As the structure is more networked, swelling will be less. The concept of constrained region also supports the swelling parameters of nanocomposites. The nanoparticle incorporation in a polymer creates interactions between the nanoparticles and the polymer chains, which are located in the vicinity of the nanoparticle.[36] These interactions cause regions with restricted chain mobility around the nanoparticles. The immobilized polymer layer (constrained zone) around the filler surface is the direct result of the effective interaction between filler and polymer. In nanocomposites, due to the presence of constrained region, the attack of solvent molecules to polymer chains will be difficult and they exhibit good solvent resistance characteristics. For the ternary hybrid systems additional filler networks and the polymer chain trapping inside it also provide superior solvent resistance.

4.6 Thermodynamics

The thermodynamics of the transport through XLPE and composites are presented in Table 4. The high heat of enthalpy, ΔH values for nanocomposites, explains the higher energy required for the diffusion process. The enthalpy value is positive, indicating that the process is endothermic. Standard enthalpy values are positive suggesting that sorption is dominated by Henry's law. The value of ΔH gives additional information about the molecular transport

through the polymer matrix. ΔH is a composite parameter involving contributions from Henry's law and Langmuir type sorption. (i) Henry's law is needed for the formation of a site and the dissolution of the species into that site-the formation of the site involves an endothermic contribution and (ii) Langmuir's (hole filling) type sorption mechanism, in which case the site already exists in the polymer matrix and sorption by hole filling gives exothermic heat of sorption. All values are positive suggesting that sorption is mainly dominated by Henry's law, *i.e.* the formation of sites and the filling of these sites by penetrant molecules. The ΔS values favour the spontaneity of the process. ΔG values are negative *i.e.* process is spontaneous for pristine XLPE and the binary nanocomposites. For ternary hybrid nanocomposites, ΔG value is positive and it represents the non-spontaneous process. This indicates the stability of the ternary hybrid nanocomposites against the solvent penetration process.

Table 4: Thermodynamic parameters of XLPE and nanocomposites of 5 wt% filler concentration

Sample	ΔH^0 (kJ/mol)	ΔS^0 (kJ/mol)	ΔG^0 (kJ/mol)
X	30.113	0.123	-3.724
A	38.579	0.144	-0.825
C	37.074	0.139	-1.037
A1C	46.637	0.164	1.603
A2C	41.842	0.152	0.226

4.7 Transport Kinetics

The first order kinetic model has been used to follow the kinetics of diffusion of solvents through XLPE/inorganic hybrid nanocomposites. In order to apply this model it is assumed that during the sorption of solvents, structural changes may occur in polymer chains, which require a rearrangement of the polymer segments that can dominate the kinetic behaviour.[37] Figure 11 shows the plot of log (C_∞ - C_t) vs t for XLPE and nanocomposites in toluene. From the slope of the straight line the value of rate constant is determined and is presented in Table 5. The kinetics of diffusion was well studied by Thomas and Windle [38] and they observed that the rate-controlling step at the penetrant front is the time-dependant mechanical deformation of the polymer in response to the thermodynamic swelling stress. Southern and Thomas [39] have suggested that when an elastomeric polymer swells, in the early stages of swelling, the lateral expansion is prevented by the underlying unswollen material. This results in a two-dimensional compressive stress in the polymer surface. As the swelling continues, equilibrium swelling of the surface layer increases and compressive stress decreases and

finally reaches in an unconstrained state. Hence, the transport kinetics can be studied by first-order kinetic equation. Again the values show that the rate of transport is less for nanocomposites and it has effect on geometrical and nano dimensional difference between the fillers. The change in rate constant values of different nanocomposites are owing to the difference in the availability of the effective surface area of the filler to interact with the solvent.[40] These conclusions are supported by the diffusion coefficient, sorption coefficient, and permeability coefficient of the systems.

Table 5: Rate constant of XLPE and nanocomposites

Sample	Rate constant k x 10^2 min^{-1}
X	6.54
A	4.19
C	5.65
A1C	4.01
A2C	5.08

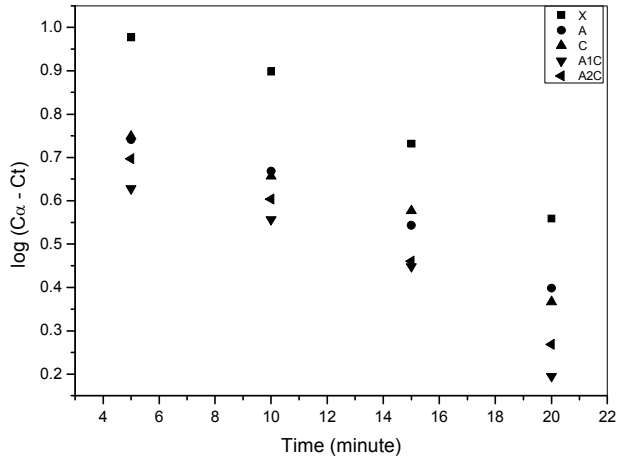

Figure 11: Plot of log (C_∞ - C_t) vs T for XLPE and nanocomposites of 5 wt% filler concentration

4.8 Theoretical Modelling

Kinetic diffusion modelling is used to analyse the diffusion behaviour through polymers, optimization of the diffusion kinetics and elucidation of the mechanism of transport, by comparing experimental data with theoretical models. Higuchi model, Korsmeyer Peppas model and Peppas-Sahlin equation were selected to predict the diffusion behaviour of the present system. All these models are based on the process in which penetrants migrate from the initial position in the polymeric system to the polymer's outer surface.[41] This is affected

by factors such as the physicochemical properties of the penetrant solvent and the structural characteristics of the material system. Penetrant diffusion and polymeric matrix swelling are suggested to be the main driving forces for transport of penetrants in polymeric matrices. Applying these models in polymeric system is thus justified.

Higuchi model

The Higuchi model [42] is represented as:

$Q_t = k_h\, t^{½}$ ……(14)

Where K_h is the Higuchi dissolution constant, t is the time and Qt is the molar percentage uptake.

Higuchi equation tries to relate the release rate based on simple laws of diffusion. The equation describes the release/diffusion processes under Fickian mechanism, or through non Fickian mechanism. In the case of Fickian mechanism, the rate of diffusion is much less than that of polymer relaxation. For Case II system or non Fickian, the rate of diffusion is much larger than that of polymer relaxation.

Korsmeyer-Peppas model

The Korsmeyer-Peppas model [43] is represented as:

$M_t/M_\alpha = k\, t^n$ ……(15)

Where M_t/M_α is the fraction of solvent released at time t, k is the constant characteristic of filler-polymer system, and n is the diffusion exponent. From the equation it can be related that the fractional diffusion is exponentially related to diffusion time.

Peppas and Sahlin model

The Peppas and Sahlin model [44] is represented as:

$M_t/M_\alpha = K_f\, t^m + K_r\, t^{2m}$ …… (16)

Where M_t/M_α is the fraction of solvent released at time t, K_f is the diffusion Fickian contribution coefficient, K_r is the relaxation contribution coefficient and m is the purely Fickian diffusion exponent.

Peppas and Sahlin model predicts the mechanism that considers diffusion in polymer matrices as a result of two processes, *i.e.* diffusion into the swollen polymer and matrix relaxation.

Experimental and theoretical model fitting values are plotted in Figure 12 and the correlation coefficient and other parameters of different modelling are given in Table 6. Among the theoretical models, Peppas Sahlin model fitted well for the experimental values, which implies that the diffusion process is considered to be the combination of diffusion into the swollen polymer and the polymer relaxation process. The selection of the appropriate model to ensure the effectiveness can be found out from correlation coefficient (R) (Table 6) and it is found that the experimental value fitted quite well into the model.

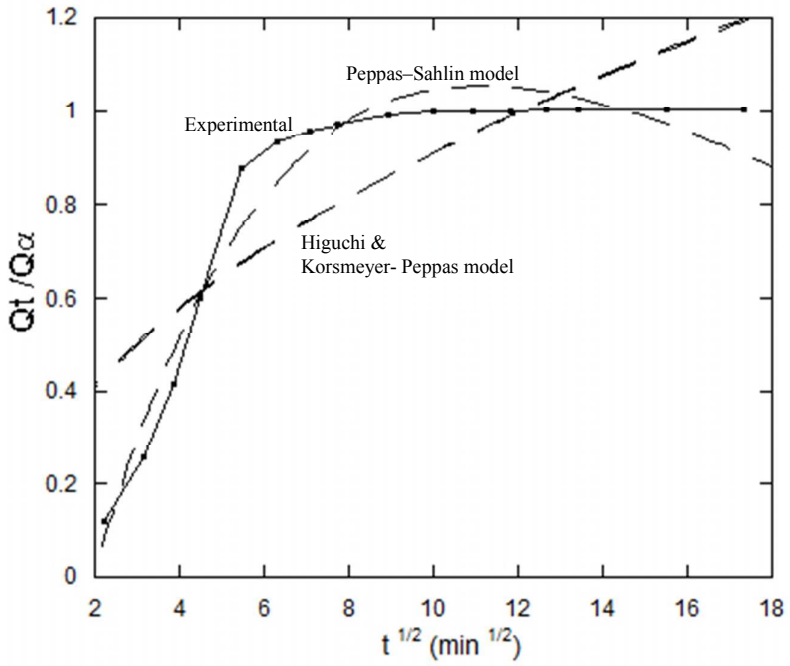

Figure 12: Model fitting of the solvent penetration through XLPE/5wt% Al_2O_3 nanocomposite (A) using Peppas–Sahlin, Haguchi and Korsmeyer- Peppas

Table 6: Correlation coefficient (R^2) and parameters of different kinetic models

Sample	Peppas Sahlin model			korsmeyer-Peppas model		Haguchi model	
XLPE/5 wt% Al_2O_3 A	R^2	K_f	K_r	R^2	n	R^2	k
	0.96	4.88	-5.66	0.683	0.5	0.684	0.28

4.9 Tensile Test at 120 ^oC

The morphological and micro-structural control over transport characteristics is further confirmed by the network density estimation by the stress-strain behaviour above the melting temperature.

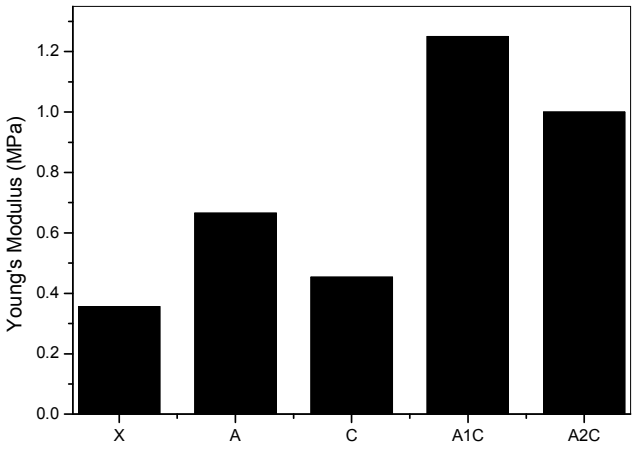

Figure 13: Plot of Young's modulus at 120 ^{0}C with different fillers of same concentration (5 wt%)

From the stress-strain behaviour, above the melting temperature, the modulus value could be computed [Figure 13]. This modulus value will be the direct result of the network structure of the system, as the crystalline fraction melts at this temperature, which is the main contributor of the modulus value of semi crystalline polymers below its melting temperature. Total network density is the sum of chemical cross links and physical networks. Nanoparticles can contribute towards both chemical cross links and physical networks by immobilized polymer fractions.[45] The network density results confirm the role of hybrid fillers in network formation and there by trapping mechanism, as the modulus value is very high for Al_2O_3:clay = 1:1nanocomposite compared to other systems. The two ternary systems show higher values than the binary systems, which are superior to the neat polymer. This is due to the synergism between the fillers, which shows maximum efficiency at Al_2O_3: clay = 1:1. For a system of 2:1 ratio of hybrid fillers, due to the excess alumina concentration, self-aggregation dominates over the interaction between alumina and clay platelets.[46] This shows the network formation ability of A2C is less than that of A1C composite, but higher than that of binary composites of alumina or clay alone systems.

All the reinforced systems show superior network density compared to the neat XLPE. For the binary system, the network density enhancement can be correlated to the formation of constrained zone, a regions with restricted chain mobility around the nanoparticles while for the hybrid ternary system; it is the sum of the trapped polymer chains in the filler networks and the constrained zone.[47,48] In the present system of XLPE/Al_2O_3/clay ternary hybrid systems, the presence of efficient filler networks trap and protect the polymer chains and this answers for the superior solvent resistant characteristics of ternary systems, especially Al_2O_3: clay = 1:1 system. As the system is more effectively packed with fillers, polymer chain dynamics is highly restricted which oppose the solvent penetration even at high temperature regions. The reduced segmental mobility and availability of minimum free volume favours

the diffusion properties of ternary system. As the nanofiller is well dispersed in the XLPE, it contributes to the network density by physical adsoption of polymeric chains on nanofillers for binary systems, which makes a tortous travel path to the solvent molecules and thus resist its penetration.

5. Conclusions

Transport properties of hybrid nanoparticle based XLPE/Al_2O_3/clay binary and ternary nanocomposites have been investigated with special significance to the self-assembling hybrid filler effect and its effect on polymer chain dynamics and accordingly its influence on transport mechanism. While comparing different nanocomposites of same filler concentration, solvent uptake is least for Al_2O_3/clay (1:1) ternary hybrid nanocomposite A1C, followed by hybrid composite of A2C (Al_2O_3/clay in 2:1 ratio) and the binary nanocomposites. In ternary hybrid composites, effective filler/filler networks can trap the polymer chains and thus the polymer segmental mobility has been reduced to a large extent. Also, due to the synergism of nanofillers of Al_2O_3 and clay, filler networks are strong and the polymer/filler interaction is also superior to binary systems. The amount of polymer chains immobilized by the filler surface has been computed form dynamic mechanical analysis and a nice correlation was established between transport characteristics and the polymer chain confinement. For hybrid nanocomposites 'n' values (mechanism of transport) are in the range of super case II and anomalous transport indicating that the time taken by polymer segments to respond to swelling stress and rearrange them to accommodate the solvent molecules is very high. Transport coefficient values and the swelling parameter confirm the superior solvent resistance property of the nanocomposites, especially ternary system of 1:1 ratio (A1C), in which the microstructure assisted diffusion mechanism control the solvent penetration process. Thermodynamics suggest that the sorption is mainly dominated by Henry's law*i.e.*first the diffusion sites are formed and then these sites are filled by penetrant molecules. Transport process, follows first order kinetics and the rate constant values again confirm the superior solvent resistant characteristics of nanocompositesparticularly A1C. Among different theoretical models, Peppas Sahlin model fitted well for the experimental values, which implies that the diffusion process is considered to be the combination of diffusion into the swollen polymer and the polymer relaxation process.

6. References

1. H. F. Kudina, A. I. Burya, *International Scientific Conference*, 19-20 November 2010**,** Gabrovo
2. M. S. Sreekala, J. George, M. G. Kumaran, S. Thomas, *Comp. Sci. Tech.* 2002, **62**, 339
3. J. Fritzsche, H. Lorenz, M. Kluppel, *Macromol. Mater.Eng.* 2009, **294**, 551-560
4. M. N. Muralidharan, S. Anil Kumar, S. Thomas, *Journal of Membrane Science,* 2008, **315**, 147–154
5. H. J. Maria, N. Lyczko, A. Nzihou, C. Mathew, S. C. George, K. Joseph, S. Thomas, *J. Mater. Sci,* 2013, **48**, 5373-5386
6. R. Wilson, S. M. George, H. J. Maria, S. T. Plivelic, A. Kumar, S. Thomas, *J. Phys. Chem.*

C. 2012, **116**, 2002-2014
7. D. P. N. Vlasveld, J. Groenewold, H. E. N. Jbersee, S. J. Picken, *Polymer,* 2005*,* **46**, 12567-12576
8. Z. M. Liang, J. Yin, *Journal of Applied Polymer Science* 2003, **90**, 1857-1863
9. Z. I. Liang, J. H. Wu, Z. X. Qiu, F. F. He, *European Polymer Journal* 2004, **40**, 307-314
10. A. Singh, M. Mukherjee, *Macromolecules* 2005, **38**, 8795-8802
11. T. M. Aminabhavi, H. T. S. Phayde, *Polymer* 1995, **36**, 1023
12. J. Chiou, D. R. Paul, *Polym. Eng. Sci*. 1986, **26**, 1218
13. W. R. Vieth, Diffusion in and through Polymers. Oxford University Press, New York, 1991
14. S. Joseph, S. Thomas, K. Joseph, U. Cvelbar, P. Panja, M. Ceh, *Journal of Adhesion Science and Technology* 2012, **26**, 271-288
15. P. C. Thomas, J. E. Tomlal, P. T. Selvin, S. Thomas, K. Joseph, *Polym. Compos*. 2010, **31**, 1515-1524
16. K. A. Molly, S. S. Bhagawan, S. C. George, S. Thomas, *J. Mater. Sci*. 2007, **42**, 4552-4561
17. G. J. V. Amerongen, *J. Polym. Sci.* 1950, **5**, 307-332
18. C. Kumnuantip, N. Sombatsompop, *Mater. Lett.* 2003, **57**, 3167-3174
19. H. C. Obasi, O. Ogbobe, I. O. Igwe, *Int. J. Polym. Sci*., 2009
20. K. C. Manoj. K. Kumari, C. Rajesh, G. Unnikrishnan, *J. Polym. Res*. 2010, **17**, 1-9
21. G. Unnikrishnan, S. Thomas, *J. Appln. Polym. Sci.* 1996, **60**, 963
22. G. Polizos, V. Tomer, E. Manias, C. A. Randall, *Journal of applied Physics*, 2010, **108**, 074117
23. S. N. Leung, M. O. Khan, E. Chan, H. E. Naguib, F. Dawson, V. Adinkrah, L. L. Hayward, *J. Appl. Polym. Sci*. 2013, **10**, 3293-3301
24. R. Stephen, S. Varghese, K. Joseph, Z. Oommen, S. Thomas, *Journal of Membrane Science* 2006, **282,** 162–170
25. A. Das, K. W. Stockelhuber, S. Rooj, D. Y. Wang, G. Heinrich, *Raw Materials and Application* 2010, 296-302
26. J. Li, P. S. Wong, J. K. Kim, *Materials Science and Engineering A*, 2008, **483** , 660-663
27. A. P. Meera, S. Said, Y. Grohens, S. Thomas, *J. Phys. Chem. C.* 2009, **113**, 17997-18002
28. Y. Rao, J. M. Pochan, *Macromolecules,* 2007, **40**, 290-296
29. P. Vijayan, D. Puglia, J. M. Kenny, S. Thomas, *Soft Matter*, 2013, **9**, 2899-2911
30. P. C. Thomas, S. P. Thomas, G. George, S. Thomas, K. Joseph, *J. Polym. Res.* 2011, **18**, 2367
31. S. C. George, S. Thomas, *Prog. Polym. Sci.* 2001, **26**, 985-1017
32. L. Mathew, K. U. Joseph, R Joseph,. *Bull. Mater. Sci*. 2006, **29**, 91–99
33. S. Jose, S. Thomas, *J. Appl. Polym. Sci*. 2001, **82**, 2404
34. F. Aviles, A. M. Montero, *Polym. Compos*. 2010, **31**, 714
35. R. Stephen, K. Joseph, Z. Oommen, S. Thomas, *Compos. Sci. Technol*. 2007, **67**, 1187
36. T. P. Selvin, J. Kuruvilla, S. Thomas, *Materials Letters,* 2004, **58,** 281-289
37. P. V. Anil Kumar, S. Anilkumar, K. T. Varughese, S. Thomas, J. Polym. Res. 2012, **19**, 9794
38. N. L. Thomas, A.H. Windle, *Polymer*, 1977, **18**, 1195

39. E. Southern, A. G. Thomas, *J. Polym. Sci. A General Papers* 1965, **3**, 641
40. D. Kim, J. M. Caruthers, N. A. Peppas, *Macromolecules,* 1993, **26**, 1841–1847
41. T. P. Selvin, J. Kuruvilla, S. Thomas, *Materials Letters,* 2004, **58**, 281-289
42. T. Higuchi, *J. Pharm. Sci.* 1963, **52**, 1145–1149
43. R. W. Korsmeyer, R. Gurny, E. Doelker, P. Buri, N. A. Peppas, *Int J Pharm* 1983, **15**, 25–35
44. N. A. Peppas, J. Sahlin, *J. Int J Pharm* 1989, **57**, 169–172
45. A. A. K. Chuk, A. N. Shchegolikhin, V. G. Schvchenko, P. M. Nedorezova, A. N. Klyamkina, M. Aladyshev, *Macromolecules*, 2008, **41**, 3149-3156
46. J. P. Jose, V. Mhetar, S. Culligan, S. Thomas, *Science of Advanced Materials,* 2013, **5**, 1-12
47. J. P. Jose, S. Thomas *Phys. Chem. Chem. Phys.,* 2014, **16**, 14730—14740
48. J. P. Jose, L. Chazeau, J. Y. Cavaille, K. T. Varughese, S. Thomas, *RSC Adv.*, 2014, **4**, 31643–31651